

Short Communication

Exploring the adhesion properties of extracellular vesicles for functional assays

Bianca C. Pachane^{1,2}, Bess Carlson¹, Suzanne E. Queen¹, Heloisa S. Selistre-de-Araujo²,
Kenneth W. Witwer^{1*}

¹ Department of Molecular and Comparative Pathobiology, Johns Hopkins University School of Medicine, Baltimore, MD, USA.

² Biochemistry and Molecular Biology Laboratory, Department of Physiological Sciences, Universidade Federal de São Carlos – UFSCar, São Carlos, SP, Brazil.

* Corresponding author:
E-mail: kwitwer1@jhmi.edu

ORCID:

BCP: 0000-0002-7302-4498

HSSA: 0000-0002-2372-7814

KWW: 0000-0003-1664-4233

22 **Abstract**

23 The “stickiness” of extracellular vesicles (EVs) can pose challenges for EV processing and
 24 storage, but adhesive properties may also be exploited to immobilize EVs directly on surfaces
 25 for various measurement techniques, including super-resolution microscopy. Direct adhesion
 26 to surfaces may allow examination of broader populations of EVs than molecular affinity
 27 approaches, which can also involve specialized, expensive affinity reagents. Here, we report
 28 on the interaction of EVs with borosilicate glass and quartz coverslips and on the effects of
 29 pre-coating coverslips with poly-L-lysine (PLL), a reagent commonly used to facilitate
 30 interactions between negatively charged surfaces of cells and amorphous surfaces.
 31 Additionally, we compared two mounting media conditions for super-resolution microscopy
 32 (SRM) imaging and used immobilized EVs for a B-cell interaction test. Our findings suggest
 33 that borosilicate glass coverslips immobilize EVs better than quartz glass coverslips. We also
 34 found that PLL is not strictly required for EV retention but contributes to the uniform
 35 distribution of EVs on borosilicate glass coverslips. Overall, these findings suggest that
 36 standard lab materials like borosilicate glass coverslips, with or without PLL, can be
 37 effectively used for the immobilization of EVs in specific imaging techniques.

38

39 Keywords: Extracellular vesicles; super-resolution microscopy; adhesion.

40

41 **Introduction**

42 Extracellular vesicles (EV) adhesive properties arise from phenomena including charge (the
 43 EV surface is usually negatively charged) and molecular affinities due to the presence of,
 44 e.g., integrins and other adhesion molecules (1). Multiple studies have investigated EV
 45 interactions with specific materials, often in hopes of reducing negative consequences such as

46 loss to surfaces during EV storage (2–4). However, direct immobilization of EVs onto
47 materials such as glass might also allow for the improvement of techniques including
48 fluorescence microscopy.

49 Traditionally, EVs have been captured for imaging using molecular affinity reagents such as
50 antibodies (5,6). Alternatively, glass slides and coverslips can also be coated with poly-L-
51 lysine (PLL) or poly-D-lysine (PDL). As polymerized amino acids with cationic charge, these
52 reagents enhance the capture of negatively charged particles (7,8).

53 Non-specific immobilization may be especially valuable now that super-resolution (SRM)
54 has evolved to enable semi-quantitative multiplexed single-molecule characterization of the
55 composition of single EVs and thus convey a richer sense of EV heterogeneity (9). For this
56 reason, we investigated several aspects of EV immobilization onto surfaces for imaging. We
57 tested the direct adherence of EVs onto borosilicate glass and quartz coverslips, further
58 probing the extent to which pre-coating with PLL enhances EV immobilization. We also
59 examined mounting conditions for SRM imaging and determined that glass-immobilized EVs
60 could also be used for cell interaction assays. We submit that these findings will be valuable
61 for other investigators who wish to image immobilized EVs.

62 **Materials and Methods**

63 **EV production: cell culture and transfection and EV separation**

64 Using the Expi293TM expression system (Gibco #A14635), Expi293F cells were grown and
65 transfected with the pLenti-palmGRET reporter plasmid (Addgene #158221) (10) following
66 the manufacturer's instructions, as described previously (11). Three days after transfection,
67 the cell suspension was centrifuged at $300 \times g$ for 5 min to remove cells from the conditioned
68 medium. For Expi293F-palmGRET EV separation, the conditioned medium was centrifuged
69 at $2,000 \times g$ for 20 min, filtered through a 0.22 μm bottle-top system (Corning), and

70 concentrated 10X by tangential flow filtration (TFF, Vivaflow[®] 50R TFF cassettes,
71 Sartorius). Samples were further concentrated 4X using ultrafiltration (Centricon Plus 70
72 Ultracel[®] PL-100, Merck Millipore; 4,000 × g, 20 min, RT) and eluted (1,500 × g, 2 min).
73 Samples were separated into 11 fractions using size-exclusion chromatography (SEC; qEV10
74 70nm columns, IZON). EV-enriched fractions (1-4) were pooled and concentrated using
75 Amicon 15 Ultra RC 10 kDa MWCO filters (Merck Millipore). Expi293F-palmGRET EV
76 aliquots in Dulbecco's phosphate buffered saline (DPBS) were stored at 4 °C for short-term
77 use and at -80 °C for long-term storage.

78 **Western blotting**

79 Expi293F-palmGRET cells were harvested and washed twice in DPBS (2,500 × g, 5 min,
80 RT). The resulting pellet was lysed with RIPA buffer (Cell Signaling Technology #9806) for
81 1 h on ice, vortexing every 15 minutes. The cell lysate was centrifuged at 14,000 × g for 15
82 min at 4 °C to remove debris, and the supernatant was quantified using BCA protein assay
83 (Thermo Scientific #23227). EV samples and SEC fractions (10 µl) were lysed with RIPA
84 buffer for 10 min at room temperature. Samples were mixed with reducing (Thermo
85 Scientific #39000) or non-reducing (Thermo Scientific #39001) sample buffer, boiled at 100
86 °C for 5 min, and loaded into Criterion TGX stain-free gels (4-15%; Bio-Rad #5678084) with
87 a Spectra[™] Multicolor Broad Range Protein Ladder (Thermo Fisher #26634). Gels ran in
88 Tris/Glycine/SDS buffer (Bio-Rad #1610772) at constant voltage (100V) for 1.5 h, and stain-
89 free gels were imaged on the Gel Doc EZ imager (Bio-Rad). Proteins were transferred to
90 PVDF membranes (iBlot[™] 2 Transfer Stacks, Invitrogen #IB24001) on the iBlot[™] 2 Gel
91 Transfer Device (Invitrogen) using a stacked program (20 V for 1 min; 23 V for 4 min, and
92 25 V for 2 min). Membranes were blocked with 5% milk-PBST for at least 1 h at room
93 temperature under agitation and incubated with primary antibodies overnight at 4 °C with
94 orbital shaking. Membranes were probed for CD63 (1:3000, Ms, BD #556016), CD9 (1:3000,

Ms, BioLegend #312102), syntenin (1:1000, Rb, Abcam #133267) and calnexin (1:1000, Rb, Abcam #22595), washed four times with 5% milk-PBST for 5 min under agitation, and exposed to the appropriate secondary antibody (m-IgGκ BP-HRP, 1:5000, Santa Cruz #616102 or Mouse anti-Rb IgG HRP, 1:5000, Santa Cruz #2327) for 1 h, RT under agitation. Membranes were washed four times with PBST, exposed for 60 seconds to SuperSignal™ West Pico ECL substrate (Thermo Scientific #34578), and documented using the iBright 1500 (Invitrogen).

Flow nanoanalyzer

Expi293F-palmGRET EV preparations were measured for particle concentration, size distribution, and EGFP incidence (%) using a Flow NanoAnalyzer (NanoFCM Co., Ltd). System start-up included laser alignment and calibration with fluorescent 250 nm silica nanoparticles (2.19E+10 particles/ml, NanoFCM #QS2503) for particle concentration and a premixed silica nanosphere cocktail with monodisperse nanoparticle populations of 68 nm, 91 nm, 113 nm, and 155 nm in diameter (NanoFCM #516M-Exo) for size dispersion. Blank was set with DPBS as the vehicle. EV samples were diluted 1:1000 (v/v) in DPBS and boosted for 60 seconds before particle signal acquisition, using constant pressure of 1 kPa and event rates between 1,500 and 10,000 events/min. Signals for side-scattering and EGFP signal, particle concentration, and size dispersion were calculated using NanoFCM Professional Suite V2.0 software.

Transmission electron microscopy

Expi293F-palmGRET EV stock was diluted 1:20 (v/v) and adsorbed to glow-discharged carbon-coated 400 mesh copper grids by flotation for 2 min. Grids were quickly blotted and rinsed by floatation on three drops of Tris-buffered saline, 1 min each, before being negatively stained in two consecutive drops of 1% uranyl acetate (UAT) with tylose (1% UAT in deionized water (diH₂O), double filtered through a 0.22-μm filter). Grids were

blotted and quickly aspirated to cover the sample with a thin layer of stain. Grids were imaged on a Hitachi 7600 transmission electron microscope (TEM) operating at 80 kV with an AMT XR80 CCD (8 megapixel), under magnification ranging from 30,000x to 120,000x.

Coverglass chamber preparation for EV immobilization

Schott D 263[®] coverglass chambers (μ -Slide 8 Well high Glass Bottom, ibidi #80807) were coated with 300 μ l of poly-L-lysine solution (0.1% PLL in H₂O (w/v), Sigma #P8920) and incubated overnight at 4 °C. The coating residue was removed through two washes with 500 μ l of DPBS (Gibco). Expi293F-palmGRET EVs (4E+08 particles/ml in DPBS, 300 μ l per well) were used to coat both PLL-coated and uncoated chambers and were incubated overnight at 4 °C and protected from light. The next day, wells were washed with DPBS twice (300 μ l per well) and filled with either 300 μ l of DPBS or 100 μ l of VECTASHIELD[®] mounting medium (Vector Laboratories #H-1000-10). Samples were stored at 4 °C until analysis. Three independent repeats with technical duplicates were done.

Coverslip preparation for EV immobilization

Borosilicate glass coverslips (Carolina Cover Glasses, Circle 12 mm, Thickness 0.13-0.17 mm, Carolina Science & Math #NC9537307) and quartz coverslips (\varnothing 10mm x 0.25mm thick, Ted Pella #26010) were rinsed with 70% ethanol and dried before use. Placed atop a 30 μ l drop of EV dilution (4E+08 particles/ml) on parafilm, coverslips were incubated overnight at 4 °C, protected from light. Coverslips were rinsed twice with DPBS and placed onto clear histological slides using VECTASHIELD[®] mounting medium. Slides were sealed (CoverGrip Coverslip Sealant, Biotium #23005) and stored at 4 °C until analysis. The experiment was conducted with two slips per group, in three independent repeats, using two distinct EV preparations.

Direct stochastic optical reconstruction microscopy (dSTORM)

A super-resolution microscopy system (Nanoimager, Oxford NanoImaging), coupled with NimOS software, was calibrated using beads detected using 405/473/532/635 nm laser excitation, mounted atop a 100x oil-objective lens. Good quality channel mapping calibration was obtained through adequate point coverage. Coverslips and coverglass chambers were imaged in seven random sites ($79.28 \mu\text{m} \times 49.43 \mu\text{m}$) with 1000 frames at 30 ms exposure and 1.4 numerical aperture. Laser intensity was optimized for each sample. Post-acquisition spatial analysis was performed using CODI (alto.codi.bio), using the “clustering and counting” app for correcting drift, clustering populations, and counting particles. Widefield images were acquired under 1x zoom, and reconstituted images were snapped acquired under 6-8x zoom.

B cell isolation

Non-human primate samples were obtained from SPF juvenile male pigtailed macaques (*Macaca nemestrina*) in procedures approved by the Johns Hopkins University Animal Care and Use Committee (ACUC) and conducted following the Weatherall Report, the Guide for the Care and Use of Laboratory Animals, and the USDA Animal Welfare Act. Blood samples were diluted (1:1, v/v) in Hank’s balanced salt solution (HBSS) and applied to SepMate™-15 (IVD) tubes loaded with a density gradient (Percoll®, Cytiva #17-0891-01). Blood was spun at $1,200 \times g$ for 10 min for separation into three phases, and the upper fraction, containing mononuclear cells (MNC), was transferred to fresh tubes and washed with HBSS. Cells were pelleted ($300 \times g$ for 8 min) and treated with red blood cell lysis buffer (ACK lysing buffer 0.83% NH_4Cl , 0.1% KHCO_3 , 0.03% EDTA) for 10 min at 37 °C. Cells were washed with HBSS, spun at $300 \times g$ for 8 min, and resuspended in cold selection buffer (PBS + 0.5% BSA + 2 mM EDTA) mixed with 20% (v/v) CD20 MicroBeads (Miltenyi Biotec #130-091-104 and #130-042-201) for 15 min at 4 °C. The suspension was diluted in selection buffer, centrifuged at $300 \times g$ for 8 min, resuspended in buffer, and applied onto MS columns

(Miltenyi Biotec #130-042-201) for magnetic cell sorting using MiniMACS™ separators (Miltenyi Biotec). CD20⁺ B cells were collected in conical tubes, pelleted (300 × g for 8 min), and resuspended in RPMI 1640 + 10% FBS + 1% pen/strep for cell counting.

B cell adhesion to EV coating

Coverglass chambers (μ-Slide 8 Well high Glass Bottom, ibidi #80807) were coated with 300 μl poly-L-lysine (PLL, 0.1%, v/v) for 2 h at 4 °C and washed with DPBS (300 μl/well). An EV suspension (4E+08 particles/ml in DPBS) was used to coat wells overnight at 4 °C, protected from light. Wells coated with 1% BSA-PBS (200 μl/well) were used as the negative control. Excess coating was washed off with 300 μl DPBS, and non-specific binding was blocked with 300 μl 1% BSA-PBS in each well, followed by a 1-hour incubation at 37 °C. B cells (1E+05 cells in 300 μl RPMI 1640 10% FBS) were applied to each well and incubated at 37 °C, 5% CO₂, for 1 h. Unbound cells were removed with three washes with DPBS (300 μl per well) before fixation with 4% PFA for 10 min at RT. Cells were washed twice with PBS, permeabilized with 0.1% Triton X-100 for 5 min at RT, and washed again. F-actin was stained with Phalloidin-647 (200 μl/well, 1:1000 dilution in PBS, Abcam #176759) for 1 h in the dark, and excess dye was washed off twice with PBS. Wells were coated with Prolong Mounting Medium with DAPI and sealed with parafilm for analysis using the Nanoimager (ONI). Cell count was assessed via nuclei count using FIJI (ImageJ), imaging a minimum of 6 random sites under 20x magnification using a confocal microscope (Zeiss 880 Airyscan FAST). The experiment was conducted on two independent occasions, using duplicated wells per group in each repeat.

Statistical analysis

Raw data were checked for outliers using the ROUT method (12), assuming a Q = 0.1. D'Agostino-Pearson omnibus K2 normality test was applied to identify data distribution. Parametric data were analyzed using unpaired t-test or one-way ANOVA with Tukey's

multiple comparison test, and non-parametric data were analyzed using the Mann-Whitney test. Statistical analysis and graphs were executed on GraphPad Prism (v. 10.0.1 (170)).

Results

Expi293F-palmGRET EV characterization

Expi293F cells were cultured to 720 ml of culture. Approximately 2.8×10^9 cells were transfected with pLenti-palmGRET EGFP-nanoluciferase reporter plasmid. Transfection efficiency was estimated under a fluorescent microscope equipped with a 488nm filter on the first and third days of transfection (Fig. 1A). Cells reached a population of approximately 3.8×10^9 cells after three days, at which time EV-containing conditioned culture medium was harvested and EVs were separated. Following the updated MISEV2023 guidelines (13), Expi293F-palmGRET EVs were characterized using multiple techniques. Volumetric Western blotting for proteins CD9, CD63, syntenin, and calnexin indicated the expected depletion of ER-specific calnexin and enrichment of EV-related syntenin and tetraspanins CD63 and CD9 in the early SEC fractions (Fig. 1B). Later SEC fractions were protein-enriched compared with EV fractions (Fig. 1C). EV-enriched fractions (1-4) were pooled for nanoflow analysis, revealing concentration of 4.7×10^{11} particles/ml, with 78.7% of particles being EGFP⁺ (Fig. 1D). EV size dispersion peaked at 76 nm (Fig. 1E). EVs were visualized with transmission electron microscopy (Fig. 1F) and super-resolution microscopy (Fig. 1G), showing expected size, morphology, and fluorescence.

Fig 1. Expi293F-palmGRET EV characterization (A) Fluorescence imaging of Expi293F cells tracking the three days of transient transfection with pLenti-palmGRET. Scale bar: 50 μ m. (B) Western blotting: membranes with Expi293F cell lysate and SEC fractions 1-11 were probed for calnexin (CANX), CD9, CD63, and Syntenin-1. (C) Quantification of protein content in SEC fractions 1-11. (D) Scatter plot of EV nanoflow cytometry, showing 78.7% EGFP-positivity amongst particles from the pooled SEC fractions 1-4. (E) Size

distribution plot of Expi293F-palmGRET EVs by nanoflow cytometry. (F) Transmission electron microscopy. Scale bar: 100 nm. (G) Super-resolution microscopy image of a single EV particle emitting EGFP fluorescence. Scale bar: 50 nm.

EV immobilization is more efficient on glass than on quartz coverslips

Using the protocol depicted in Figure 2A, we found that both quartz and borosilicate glass can immobilize EVs. To count particles, each coverslip was imaged in at least six random sites in dSTORM, and the CODI software clustered signals from the multiple frames to identify individual EVs. Particle count detected 59.62 ± 17.67 on the quartz coverslip and 289.7 ± 172.3 clusters on the borosilicate glass coverslip, indicating a statistically significant difference in EV immobilization ($p < 0.0001$) (Fig. 2B). Inspection of the rendered images indicates the density of particles per frame (Fig. 2C).

Fig 2. EV immobilization on glass and quartz coverslips. (A) Experimental scheme for the preparation of EV-coated coverslips for SRM imaging. (B) Comparison of particle count between quartz and glass coverslips, obtained using the CODI software (alto.codi.bio). Non-parametric data was compared using the Mann-Whitney unpaired t-test, and the p -value is displayed on the graph. (C) Representative images of rendered dSTORM frames, showing individual Expi293F-palmGRET EVs in green, obtained at 60x magnification and 2x zoom. Scale bar: 20 μ m.

EV immobilization is more uniform with PLL pre-coating

Using an 8-well culture chamber assembled atop a Schott D 263 borosilicate coverslip, we cross-examined the requirement of specific mounting medium and PLL to improve EV immobilization on glass. The experimental design for this assay is shown in Figure 3A. Regarding the requirement of mounting medium to stabilize the sample for imaging in SRM,

we found a statistically significant difference between PBS *versus* mounting medium (MM) in glass surfaces only, but not in PLL-coated glass (Fig. 3B). This suggests PBS may be a viable medium for immersing samples in culture chambers for dSTORM, if used alongside PLL coating. We also found that EVs attached to borosilicate glass even without PLL coating (no PLL = 157.3 ± 144.9 clusters per site; PLL = 78.83 ± 45.26 clusters per site). However, although there were more EVs in the no PLL condition, high standard deviation (ranging from >50 to 300 particles per site) suggests that PLL facilitates a more uniform immobilization of EVs onto glass. Representative images of the rendered frames indicating the density of particles per site are shown in Fig. 3C.

Fig 3. EV immobilization onto borosilicate chamber coverglass. (A) Experimental scheme for the preparation of EV-coated chamber coverglasses for SRM imaging. (B) Comparison of particle count between uncoated wells or pre-coated with poly-L-lysine (0.1 mg/ml) prior to Expi293F-palmGRET EV immobilization and immersed in PBS or mounting medium (MM), obtained using the CODI software (alto.codi.bio). Non-parametric data were compared using the Kruskal-Wallis analysis of variance with Dunn's multiple comparison test, and the *p*-values are displayed on the graph. (C) Representative images of rendered dSTORM frames, showing individual Expi293F-palmGRET EVs in green, obtained at 60x magnification and 2x zoom. Scale bar: 20 μ m.

B cells interact with PLL/glass-immobilized EVs

We next performed a cell adhesion assay in which B-cells were allowed to interact with an EV-coated coverslip following a previous report (8). For this, we used PLL-coated glass coverslips and non-human primate (NHP) primary CD20⁺ B cells (Fig. 4A). An EV concentration of 4E+8 particles/ml was chosen from a dilution series (Fig. 4B) for subsequent comparison with a negative control (1% BSA-PBS). Although some cells bound to the

negative control wells, on average 3.3-fold more cells adhered to EV-coated wells (Fig. 4C); binding of cells was also confirmed by SRM (Fig. 4D).

Fig 4. B-cells adhere to EV coating. (A) Experimental scheme. (B) Optimization of EV coating concentration, ranging from 1E+8 to 8E+8 particles/ml. Representative images from SRM rendering indicate Expi293F-palmGRET EVs in green and were obtained at 60x magnification and 2x zoom. Scale bar: 20 μ m. (C) Average count of attached cells in 1% BSA-PBS (negative control) and EV coating after 1h of incubation, obtained through nuclei counting. Non-parametric data was compared using the Mann-Whitney unpaired t-test and the *p*-value is displayed on the graph. (D) Representative SRM images from the adhesion assay, showing EVs (green) and NHP B cells (red). Scale bar: 20 μ m.

Discussion

Recently, a paper demonstrated that EV immobilization occurs similarly in quartz glass slides and positively charged quartz slides while describing a novel plugin for particle count using standard fluorescent microscopy images (9). We tested if similar results could be found between standard borosilicate glass coverslips and quartz coverslips, but instead using dSTORM to assess particle disposition. Using EGFP⁺ EVs, a significantly higher mobilization of EVs in glass coverslips rather than quartz was observed, suggesting that the use of commercially available glass coverslips is possible for assays in which EVs need to be adsorbed by an amorphous surface. We also found that the use of PLL coating in borosilicate glass is not required but aids the uniformity of EV distribution. We believe the PLL coating may contribute to EV binding in sites where the glass surface is not as homogeneous, by creating an electrostatic potential to improve EV adhesion (14). On a side note, we also found that mounting medium is not essential for SRM analysis, and PBS can be used as stable media to store microscopy samples under immersion for short periods. To the best of our knowledge, no studies so far have investigated whether PLL is required for EV

immobilization on glass surfaces, and few have studied the interaction of EVs with different materials for functional assays.

Sample preparation for specific applications such as total internal reflection fluorescence (TIRF) microscopy and dSTORM often require refined materials that improve their optical transmittance without compromising the roughness value on the surface or the chemical resistance (14). Quartz is considered a superior material for optical transmission, however, its high softening point (1,500 °C) creates a more delicate material and a costlier product (15). A commercially available option is the standard glass coverslip, made from high-quality borosilicate glass with different sizes and thicknesses (e.g., 0.09 to 0.25 mm), which are suitable for microscopy, especially when treated with PLL in preparation for cell adhesion (16). EVs bind more efficiently to borosilicate glass than quartz, as found using dSTORM, suggesting that this material may be used for the development of new products focused on highly specific microscopy techniques.

Our findings suggest that the immobilization of EVs for highly specific imaging techniques may be achieved by using standard lab materials such as borosilicate glass coverslips. This simpler approach to dSTORM broadens the possibilities for methods and applications that can employ SRM. Also, coupled with the similarity between PBS and mounting medium to store the sample, we described a cheaper option for SRM preparation with equivalent results to costlier options.

Author's contribution

BCP: conceptualization, data curation, formal analysis, investigation, methodology, writing – original draft, writing – review and editing; BC: methodology, visualization; SEQ: methodology, visualization; HSSA: funding acquisition, supervision, writing – review and

editing; KWW: conceptualization, funding acquisition, supervision, resources, writing –
review and editing.

Acknowledgments

The authors thank members of the Witwer Laboratory, particularly Dr. Olesia Gobololova for consulting; the Retrovirus Laboratory; and the Biochemistry and Molecular Biology Laboratory for helpful suggestions and discussions.

Data availability

We have submitted all relevant data of our experiments to the EV-TRACK knowledgebase (EV-TRACK ID: EV240144) (17). The data that support the findings of this study are available from the corresponding author upon reasonable request.

Funding

This report was supported by the US National Institutes of Health through AI144997 (to KWW) and U42OD013117 (to EK Hutchinson), and by the São Paulo Research Foundation through grants 2019/05149-9, 2021/01983-4 and 2022/04146-9 (to BCP). The Witwer lab is also supported in part by NCI/Common Fund CA241694, NIMH MH118164, the Paul G. Allen Frontiers Group, and the Richman Family Precision Medicine Center of Excellence in Alzheimer's Disease at Johns Hopkins University.

Conflict of interest

KWW is or has been an advisory board member of ShiftBio, Exopharm, NeuroDex, NovaDip, and ReNeuron; holds stock options with NeuroDex; and privately consults as Kenneth Witwer Consulting. Ionis Pharmaceuticals, Yuvan Research, and AgriSciX have sponsored or are sponsoring research in the Witwer laboratory.

References

1. Jimenez L, Yu H, McKenzie AJ, Franklin JL, Patton JG, Liu Q, et al. Quantitative Proteomic Analysis of Small and Large Extracellular Vesicles (EVs) Reveals Enrichment of Adhesion Proteins in Small EVs. *J Proteome Res.* 2019 Mar 1;18(3):947–59.
2. Evtushenko EG, Bagrov DV, Lazarev VN, Livshits MA, Khomyakova E. Adsorption of extracellular vesicles onto the tube walls during storage in solution. *PLOS ONE.* 2020 de dez. de;15(12):e0243738.
3. Ge Q, Zhou Y, Lu J, Bai Y, Xie X, Lu Z. miRNA in Plasma Exosome is Stable under Different Storage Conditions. *Molecules.* 2014 Feb;19(2):1568–75.
4. Görgens A, Corso G, Hagey DW, Jawad Wiklander R, Gustafsson MO, Felldin U, et al. Identification of storage conditions stabilizing extracellular vesicles preparations. *J Extracell Vesicles.* 2022 Jun;11(6):e12238.
5. Reynolds DE, Pan M, Yang J, Galanis G, Roh YH, Morales RTT, et al. Double Digital Assay for Single Extracellular Vesicle and Single Molecule Detection. *Advanced Science.* 2023;10(33):2303619.
6. Singh RK, Santos MF, Herndon C, Gieler BA, Lee I, Chen J, et al. Detection by super-resolution microscopy of viral proteins inside bloodborne extracellular vesicles. *Extracell Vesicles Circ Nucleic Acids.* 2023;4(4):557–67.
7. Yu C, Zhao W, Duan C, Xie J, Yin W. Poly-l-lysine-caused cell adhesion induces pyroptosis in THP-1 monocytes. *Open Life Sci.* 2022 Mar 24;17(1):279–83.
8. Altei WF, Pachane BC, dos Santos PK, Ribeiro LNM, Sung BH, Weaver AM, et al. Inhibition of $\alpha v \beta 3$ integrin impairs adhesion and uptake of tumor-derived small extracellular vesicles. *Cell Commun Signal.* 2020 Sep 25;18(1):158.
9. Schürz M, Danmayr J, Jaritsch M, Klinglmayr E, Benirschke HM, Matea C, et al. EVAnalyzer: High content imaging for rigorous characterisation of single extracellular vesicles using standard laboratory equipment and a new open source ImageJ/Fiji plugin. *J Extracell Vesicles.* 2022 Dec;11(12):12282.
10. Wu AYT, Sung YC, Chen YJ, Chou STY, Guo V, Chien JCY, et al. Multiresolution Imaging Using Bioluminescence Resonance Energy Transfer Identifies Distinct Biodistribution Profiles of Extracellular Vesicles and Exomeres with Redirected Tropism. *Advanced Science.* 2020;7(19):2001467.
11. Driedonks T, Jiang L, Carlson B, Han Z, Liu G, Queen SE, et al. Pharmacokinetics and biodistribution of extracellular vesicles administered intravenously and intranasally to *Macaca nemestrina*. *Journal of Extracellular Biology.* 2022;1(10):e59.
12. Motulsky HJ, Brown RE. Detecting outliers when fitting data with nonlinear regression – a new method based on robust nonlinear regression and the false discovery rate. *BMC Bioinformatics.* 2006 Mar 9;7(1):123.
13. Welsh JA, Goberdhan DCI, O'Driscoll L, Buzas EI, Blenkiron C, Bussolati B, et al. Minimal information for studies of extracellular vesicles (MISEV2023): From basic to advanced approaches. *Journal of Extracellular Vesicles.* 2024;13(2):e12404.
14. Schermelleh L, Ferrand A, Huser T, Eggeling C, Sauer M, Biehlmaier O, et al. Super-resolution microscopy demystified. *Nat Cell Biol.* 2019 Jan;21(1):72–84.
15. Tang T, Yuan Y, Yalikun Y, Hosokawa Y, Li M, Tanaka Y, et al. Glass based Micro Total Analysis Systems: Materials, Fabrication methods, and Applications. *Sensors and Actuators B Chemical.* 2021 Mar 1;339.
16. Mazia D, Schatten G, Sale W. Adhesion of cells to surfaces coated with polylysine. Applications to electron microscopy. *Journal of Cell Biology.* 1975 Jul 1;66(1):198–200.
17. EV-TRACK Consortium, Van Deun J, Mestdagh P, Agostinis P, Akay Ö, Anand S, et al. EV-TRACK: transparent reporting and centralizing knowledge in extracellular vesicle research. *Nat Methods.* 2017 Feb 28;14(3):228–32.

Figures

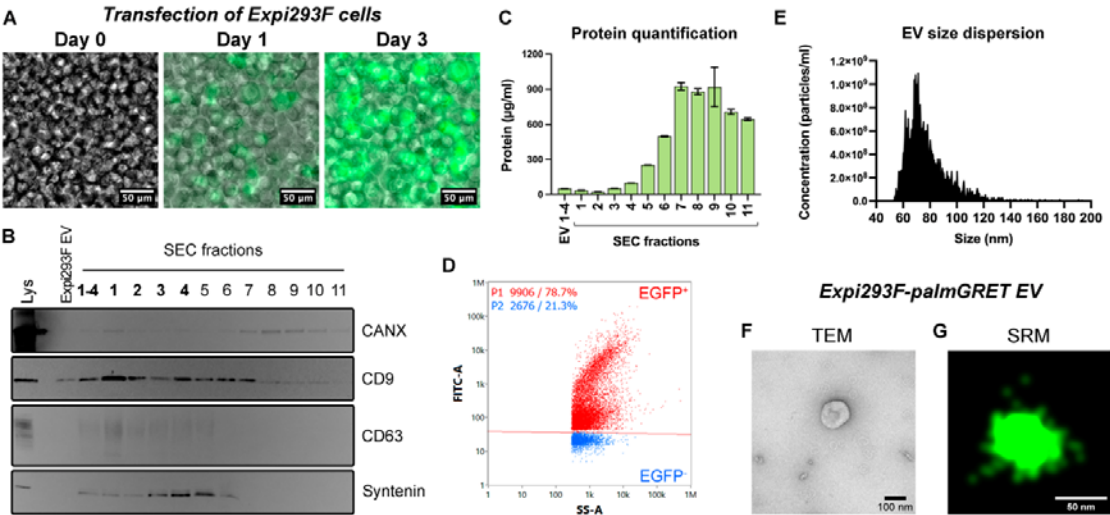


Figure 1

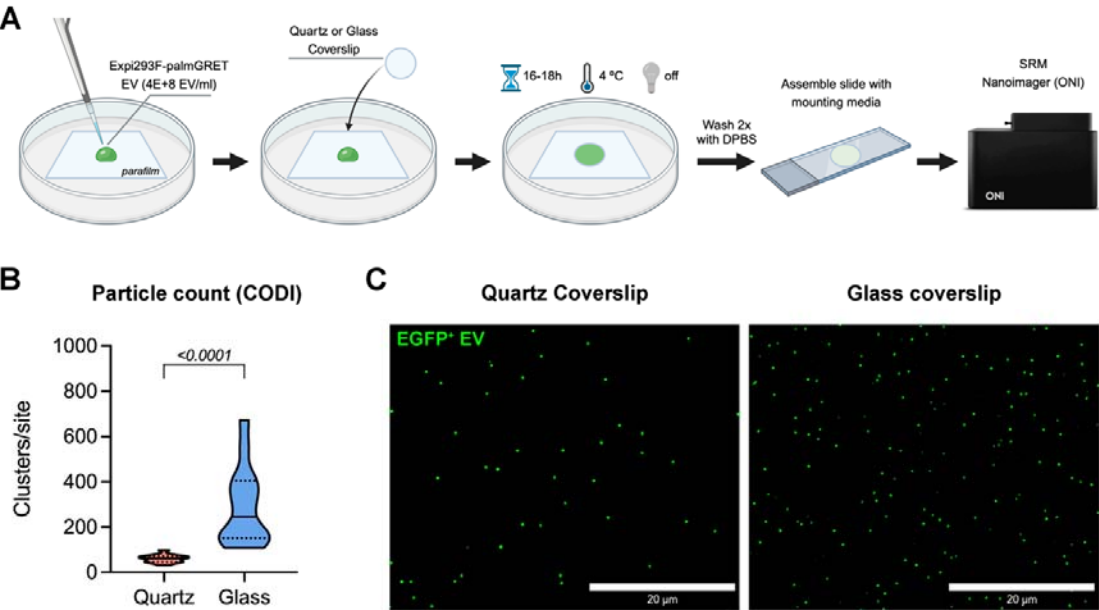


Figure 2

402

403

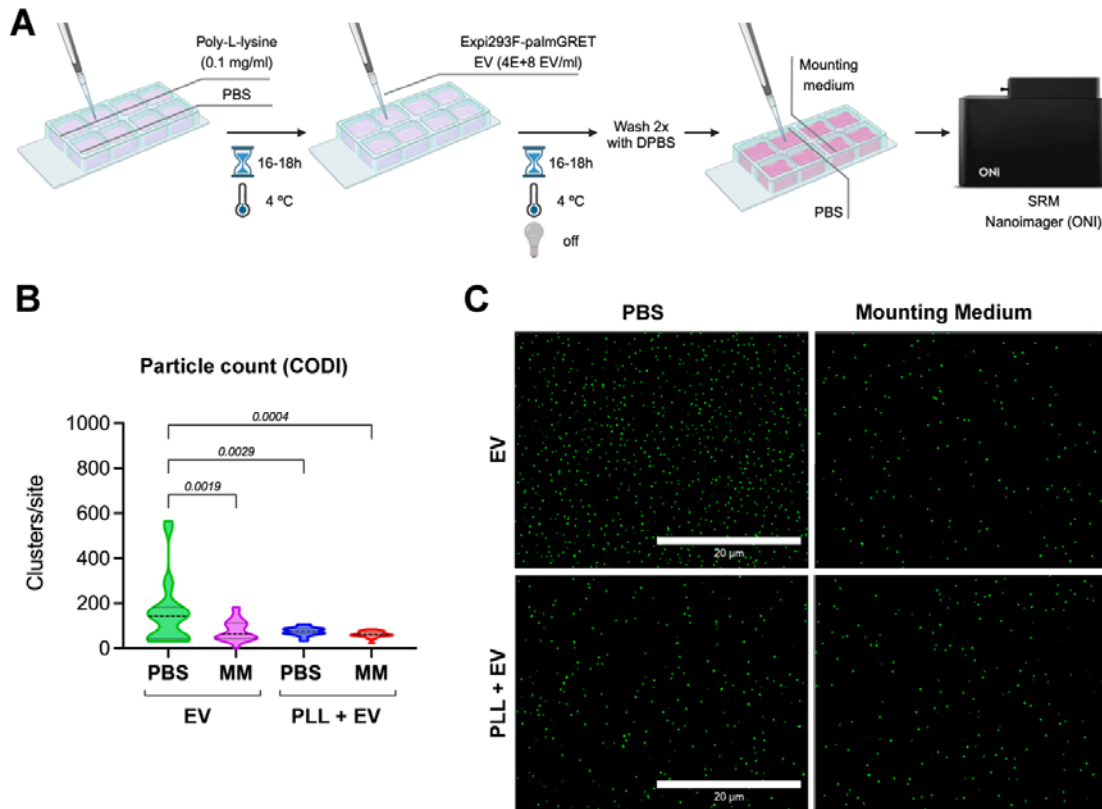


Figure 3

